Available online at www.sciencedirect.com
SCIENCE DIRECT®
Journal of Power Sources 114 (2003) 203–212
JOURNAL OF POWER SOURCES
www.elsevier.com/locate/jpowsour

On the systematic optimization of ethanol fed SOFC-based electricity generating systems in terms of energy and exergy

S.L. Douvartzides, F.A. Coutelieris, P.E. Tsiakaras*

Department of Mechanical and Industrial Engineering, University of Thessalia, Pedion Areos, 383 34 Volos, Greece

Received 5 July 2002; received in revised form 14 October 2002; accepted 28 October 2002

Abstract

An energy–exergy analysis was undertaken in order to optimize the operational conditions of a SOFC-based power plant fueled by ethanol. A certain plant configuration was contemplated, equipped with an external steam reformer, an afterburner, a mixer and two heat exchangers (preheaters). The most significant operational parameters are enunciated and their influence on the energy and exergy balances of the plant is discussed and optimized. An optimization strategy is presented and optimally controlled unit operations are specified through minimization and allocation of exergy costs.

Keywords: Systems engineering; Thermodynamics process; Optimization; SOFC systems; Energy; Exergy analysis

1. Introduction

The first law of thermodynamics invokes the energy balance between heat and work interactions of a system with its environment. However, although energy is a conserved quantity, its quality, as a measure of usefulness, is not conserved. ''Exergy'' (or ''availability'') is the part of the amount of energy at a given state that is transformable to useful work, while ''anergy'' (or ''irreversibility'') is the required wasted energy note during a process. Hence, exergy is a tool for the analysis of engineering systems aiming at the interpretation of the axiomatic role of the second law of thermodynamics and the specification of design optima unconceivable by energy conservation law. In light of this role of ''exergy analysis'', design optimization expands to cover critical aspects such as the cost-effectiveness and the environmental impact of engineering systems [1,2].

Ordinary power generation systems transform the chemical energy of a fuel into useful work (i.e. electricity) by passing through the intermediade stage of production of thermal power that is most commonly achieved by processes of combustion. This route of energy conversion results in significant losses of potential energy that could otherwise be useful in work form, because of extremely irreversible mechanisms of energy exchange between the molecules in the combustion chamber [3,4]. These mechanisms involve transfer of momentum and heat from the combustion products to the surrounding motionless species inside the chamber, being responsible for almost 70% of the entropy generation in it [3–6]. On the other hand, solid oxide fuel cells (SOFCs) are electrochemical devices operating at high temperatures (above 1000 K) that allow the conversion of the chemical energy of a fuel directly into electricity. Comprised of an oxygen ion (O^{2-}) conducting solid electrolyte and two electrodes in cathodic and anodic roles, SOFCs allow the exploitation of various fuels for generation of electricity with efficiencies unattainable by all other conventional systems [7–9]. Energy conversion takes place electrochemically through controlled migration of O^{2-} ions from the air exposed cathode to fuel fed anode and, therefore, oxidation becomes more controllable and less irreversible than in ordinary combustion systems. As a result, energy conversion and management is more rational and entropy generation is substantially lower [3,10,11].

In the present investigation, the effect of the operational conditions on the theoretical performance of a SOFC system fueled by ethanol is examined. Being the most representative renewable fuel for application in SOFCs, biomass-derived ethanol provides expectations for policies of ''green'' power generation and upgraded agricultural labor. In light of this,

Abbreviations: AHU, absolute hydrogen utilization (% per mol of ethanol); LHV, lower heating value of ethanol (1235 kJ/mol); RF, reforming factor (mole of steam/mole of ethanol); SOFC, solid oxide fuel cell

* Corresponding author. Tel.: +30-2421-074-065; fax: +30-2421-074-050.
E-mail address: tsiak@mie.uth.gr (P.E. Tsiakaras).

0378-7753/02/$ – see front matter © 2002 Elsevier Science B.V. All rights reserved.
PII: S0378-7753(02)00611-0

Nomenclature

C	thermal capacity (J/mol K)
e	specific exergy (J/mol)
emf	electromotive force (V)
E	total exergy (J)
F	Faradays' constant (96,484 J/mol V)
h	specific enthalpy (J/mol)
m	mass (kg)
p	pressure (bar)
Q	heat (J)
R	universal gas constant (8.314 J/mol K)
s	specific entropy (J/mol K)
T	temperature (K)
U	hydrogen utilization in the SOFC device (%)
W	work (J)
x	molar fraction

Greek letters

ε	extent of reforming reaction (%)
η	overall plant efficiency (%)

Supercripts

·	rate per second
e	property referred to the chemical composition of the environment
PH	index for physical exergy component
CH	index for chemical exergy component

Subscripts

0	property at the state of the environment (dead state) or for zero-loss burner balance
I	property estimated according to first law
II	property estimated according to second law
D	property destruction
gen	property generated
i	index for chemical species
j	index for individual heat transfer or index for the high temperature heat source
p	property estimated under isobaric conditions
ref	index for reformer
sofc, in	mixture incoming the SOFC device
sofc, out	mixture outcoming the SOFC device
T	property estimated under isothermal conditions
vap	index for vaporizer

the following analysis is oriented to the optimization of the overall ethanol-powered SOFC plant in terms of efficiency for generation of electrical power and exergy destruction due to irreversibilities. A mathematical model has been developed in order to simulate and optimize all processes involved [12]. Theoretical conclusions about the influence of the major operational parameters were obtained and a strategy plan aiming at the minimization of energy-exergy losses is developed.

2. Theory

2.1. Energy and exergy balances

Exergy is a thermodynamic property of a system that provides a measure of the maximum useful work that the system can attain as it is allowed to reversibly transition to a thermodynamic state in equilibrium with its environment [13,14]. Accordingly, exergy is a property dependent on both the states of the system and its environment and its calculation considers processes of thermal, mechanical and chemical character. Obviously, one may write that

$$\text{energy} = \text{exergy} + \text{anergy}. \tag{1}$$

A clarification of the exergy concept can be presented by considering a one inlet—one outlet device as a system with a flow of a mixture of i chemical species of known composition at elevated temperature and high pressure. The energy balance for this system, by ignoring the changes in kinetic and potential energies, is expressed as

$$\sum_j \dot{Q}_j - \dot{W} = \left(\sum_i \dot{m}_i h_i\right)_{\text{inlet}} - \left(\sum_i \dot{m}_i h_i\right)_{\text{exit}} \tag{2}$$

where heat flux $\dot{Q}_j$ is conventionally positive when absorbed by the system and work $\dot{W}$ is positive when it is produced by the system. On the other hand, the exergy balance for this system is,

$$\dot{E}_{\text{D}} = \left(\sum_i \dot{m}_i e_i\right)_{\text{inlet}} - \left(\sum_i \dot{m}_i e_i\right)_{\text{exit}} + \sum_j \left(1 - \frac{T_0}{T_j}\right)\dot{Q}_j - \dot{W} \tag{3}$$

where $\dot{E}_{\text{D}} = T_0 s_{\text{gen}}$ (the Gouy–Stodola theorem) represents the rate of exergy destruction into the device due to irreversibilities and e_i is the total exergy of each chemical species i. In fact, $e = \sum_i \dot{m}_i e_i$ is the sum of the physical and chemical exergy components that are associated with the physical and chemical properties of the stream of matter, respectively [14]. More precisely, physical exergy, e_i^{PH}, expresses the useful work that the chemical component i can produce if it is brought reversibly from the state of the system to the "restricted dead state" that is a state in thermal and mechanical equilibrium with the environment. Therefore, physical exergy can be expressed as,

$$e_i^{\text{PH}} = (h - h_0)_i - T_0(s - s_0)_i \tag{4}$$

where

$$(h - h_0)_i = \int_{T_0}^{T} (C_p)_i \, \mathrm{d}T \tag{5}$$

and

$$(s - s_0)_i = \int_{T_0}^{T} \frac{(C_p)_i}{T} \, \mathrm{d}T - R \ln \frac{p_i}{p_0}. \tag{6}$$

On the other hand, chemical exergy, e_i^{CH}, expresses the useful work produced by the chemical species i if it is brought reversibly from the "restricted dead state" in "dead state", which is in mechanical and in chemical equilibrium with the environment. It is apparent that the chemical species comprising the system should be referred to the properties of a suitable selected set of environmental substances. Accordingly, an appropriate "exergy reference environment" is usually used in order to estimate the standard chemical exergy e_i^{CH} according to the following relation [13–15],

$$e_i^{CH} = -RT_0 \ln \frac{x_i^e p_0}{p_0} \tag{7}$$

where x_i^e is the molar fraction of the gas i in the standard reference environment. For compounds that are not part of the environmental composition, the chemical exergy is estimated according to standard procedures described elsewhere [13]. To simulate the environment, all standard chemical exergies have been selected from literature [15] and an environmental composition of 75.67% N_2, 20.35% O_2, 0.03% CO_2, 3.03% $H_2O_{(g)}$ and 0.92% Ar was assumed in volume basis, at $T_0 = 298.15$ K and p_0=1.013 bar.

2.2. SOFC system

The flow sheet of the SOFC power plant that has been taken under consideration in the present study, is shown in Fig. 1. It is common practice to feed the SOFC with hydrogen produced by reforming of hydrocarbons or alcohol [7–9,16]. In the case of ethanol, the reaction of the steam reforming can be written as,

$$C_2H_6O + 3H_2O \rightarrow 2CO_2 + 6H_2,$$
$$\Delta H_1 = +173.536\,\text{kJ/mol of ethanol}. \tag{8}$$

It has been reported that ethanol steam reforming is possible at relatively low temperatures (at about 600 K) when assisted by appropriate catalysts [17–23].

The reformate enters in the anode compartment of the SOFC where hydrogen reacts with O^{2-} ions supplied from cathode through the solid electrolyte, as follows

$$H_2 + O^{2-} \rightarrow H_2O + 2e^-, \quad \Delta H_{H_2} = -248,818\,\text{J/mol of } H_2. \tag{9}$$

Although hydrogen oxidation is the primary reaction leading to electricity generation, in practice CO and CH_4 reformate components react also in the SOFC anode with steam (gas shift and internal reforming reactions, respectively) serving as sources for secondary hydrogen. In the present analysis, it was assumed that in the SOFC only reaction (9) takes place while a portion of unreformed ethanol is passing through the SOFC as inert gas. Accordingly, the amount of secondary hydrogen produced by CO and CH_4 was supposed as being directly fed to the SOFC inlet and was considered as parameter involving extend of reforming ε. Moreover, it was supposed that reaction (9) takes place in an extend below 100% by employing the factor of hydrogen utilization, U. In practice, a portion of hydrogen must remain as an unreacted component in the SOFC outlet to avoid potential (emf) losses in the SOFC. This can be explained by the well-known Nernst equation,

$$\text{emf} = \frac{RT}{4F} \ln \frac{p_{O_2(c)} p_{H_2(a)}^2}{p_{H_2O(a)}^2} \tag{10}$$

where the subsripts 'a' and 'c' represent states at anode and cathode, respectively. It is apparent that the electromotive force (emf) of the SOFC deteriorates significantly when hydrogen partial pressure at anode tends to zero. Moreover, a fraction of the hydrogen entering in the SOFC must be allowed to reach the afterburner in order to support the heat demands of the reformer and the vaporizer. Heat required by the reformer was set equal to $\dot{Q}_{ref} = (173{,}536\,\text{J/mol of ethanol})\varepsilon$, and that by the vaporizer was calculated as $\Delta H_{vap} = (2{,}442{,}310\,\text{J/kg of } H_2O_{(g)})\Delta \dot{m}_{H_2O_{(g)}}$ where the latent heat of water was taken, with negligible error, to correspond for vaporization at 298.15 K. These demands

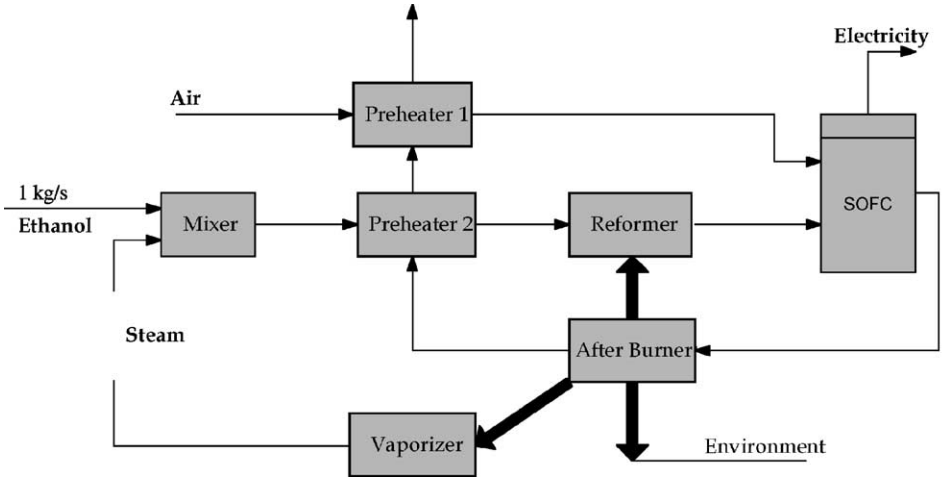

Fig. 1. Schematic representation of the SOFC power plant.

should be met by the heat produced from complete combustion of unreacted ethanol and hydrogen according to the reaction

$$C_2H_6O + 3O_2 \rightarrow 2CO_2 + 3H_2O,$$
$$\Delta H_3 = -1235\,\text{kJ/mol of ethanol} \quad (11)$$

and the oxidation of residual hydrogen according to reaction (9). Finally, as shown in Fig. 1, two preheaters (heat exchangers) were used to increase the thermal content of air before the SOFC as well as of the ethanol/steam mixture before the reformer. In order to calculate the exact temperature in each branch of the power cycle, an iterative method has been employed [24] taking into account the variation of the thermal capacities, $(C_p)_i$, with temperature.

3. Results and discussion

A mathematical model has been developed [12] in order to simulate the processes involved in the plant of Fig. 1. This simulation program was able to calculate the flow rate, the temperature, the energy and the exergy content in every stream of the matter or heat flux in the plant as well as the irriversibilities appearing in the individual units. The overall energy efficiency (η_I, %) of the plant as percentage of the chemical energy (LHV = 1235 kJ/mol) of ethanol and the overall exergy efficiency (η_{II}, %) as percentage of its standard chemical exergy of the fuel (1357.7 kJ/mol) were used as objective criteria of performance evaluation. The influence of the independent variables on the final efficiency of the system was recognized and optimized following the imminent parametric analysis.

3.1. Effect of extent of reforming, ε, and hydrogen utilization, U

As mentioned above, hydrogen oxidation in the SOFC may be regarded as the primary reaction leading to electricity generation in the plant. Hydrogen is produced by reaction (8) which is assumed to take place with an extent, ε (%), and then is oxidized according to reaction (9) with an extent, U (%). As a result, the "absolute hydrogen utilization" in the plant, AHU, may be calculated as AHU = $\varepsilon U/10000$. AHU expresses the hydrogen content per mol of ethanol supply that is exploited for power generation and, therefore, the reversible electrical work generated in the SOFC per mol of ethanol may be expressed as

$$W_{\text{el,rev}} = 6(\varepsilon U \times 10^{-4})(\Delta G_{H_2})_T = 6(\text{AHU})(\Delta G_{H_2})_T \quad (12)$$

while heat released from the SOFC reaction may be given as

$$Q = 6(\varepsilon U \times 10^{-4})[(\Delta H_{H_2})_T - (\Delta G_{H_2})_T] = 6(\text{AHU})[(\Delta H_{H_2})_T - (\Delta G_{H_2})_T] \quad (13)$$

where $(\Delta H_{H_2})_T$ and $(\Delta G_{H_2})_T$ are, respectively, the changes of enthalpy and Gibbs free energy of hydrogen oxidation at the average temperature of SOFC operation. Since $(\Delta G_{H_2})_T$ is practically unaffected by temperature variations while $(\Delta G_{H_2})_T$ decreases by temperature increment, Eqs. (12) and (13) imply that electrical work output per mol of ethanol decreases with temperature. Further, at a given temperature of SOFC operation, T, it is evident that maximization of work output is equivalent to maximization of AHU.

Although AHU maximization in the analysis of a control volume that envelopes the reformer and the SOFC devices could be considered feasible by simultaneous maximization of both extents ε and U, this is not possible when dealing with a power plant. In this case, ε and U cannot maximize simultaneously because of the requirement for positive thermal balance of the afterburner. Indeed, by assuming a standard loss of energy from the burner to environment, ΔH_{loss}, and a standard heat demand for water vaporization (i.e. a standard reforming factor, RF), ΔH_{vap}, the burner balance may be expressed, using the extents ε and U, as follows

$$\frac{\Delta H_{\text{fuel}} - \Delta H_{\text{vap}}}{6\Delta H_{H_2}} - \Delta H_{\text{loss}} = \varepsilon\left(\frac{\Delta H_{\text{fuel}} + \Delta H_{\text{ref}} - 6\Delta H_{H_2}}{6\Delta H_{H_2}} + U\right). \quad (14)$$

Eq. (14) implies that at given values of RF and ΔH_{loss}, maximization of ε corresponds to minimization of U and vise versa. As shown in Fig. 2, for a selected reforming factor equal to RF = 3, there are infinite equivalent pairs of ε and U that result in the same amount of energy loss, ΔH_{loss}, from the burner to environment. Since maximization of electrical output in the plant corresponds to maximization of AHU, the optimal design is the one of zero-loss burner balance which is represented by the locus AB of Fig. 2. At these conditions, Eq. (14) simplifies in the form

$$0.760293 = \varepsilon_0(U_0 - 0.029204), \quad 0 < \varepsilon_0 < 100\%, \quad 0 < U_0 < 99\% \quad (15)$$

where the subscript "0" indicates parameteres refered to zero-loss burner operation. Eq. (15) provides all pairs of ε_0 and U_0 leading to AHU maximization and proves that for a given ΔH_{loss} and RF, AHU is approximately constant for all pairs of ε and U (a slight increase may be observed by maximizing ε_0 instead of U_0). In other words, all pairs of the zero-loss locus AB in Fig. 2 provide approximately the same maximum AHU value and may be considered equivalent scenarios of the same optimally designed configuration when RF = 3.

From an exergetic point of view, AHU maximization at zero-loss burner conditions has a dual role of major importance in the plant optimization. Since AHU maximizes at zero-loss burner conditions, thermal exergy losses from burner are eliminated. In fact, minimization of exergy losses due to unnecessary heat waste is a constraint of great significance when the plant is designed to operate autonomously, whithout interactions with external work producing systems (turbines, heat engines, etc.). Further, AHU maximization is

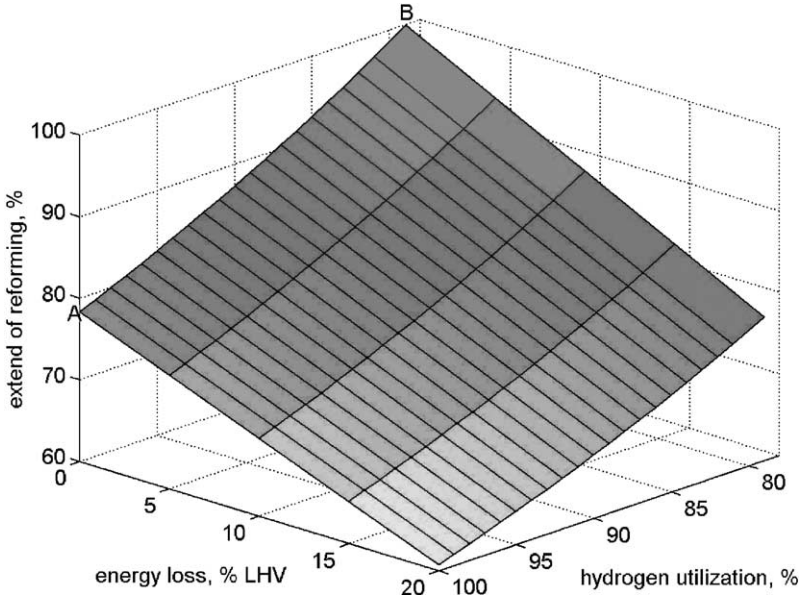

Fig. 2. Dependence of the energy balance of the burner on the extend of reforming, ε, and hydrogen utilization, U (RF = 3, curve AB corresponds to optimum extents ε_0,U_0).

by definition a constraint reflecting the maximization of the energetic role of the reformer and the SOFC and concomitantly the minimization of participation of combustion processes in the burner. As it will be proved also for the case examined in this work, spontaneous combustion is usually one of the predominant exergy sinks in the plant and significant advantages may be derived by minimizing its participation.

3.2. Effect of non-adiabatic SOFC operation

Leaving aside the optimization of the burner operation, the other device in thermal interaction with the environment is the SOFC. Accordingly, a minimization constraint must be stated also for the energy (exergy) losses due to this interaction. Given that high temperature fuel cells like SOFCs produce electrical work due to electrochemical oxidation and a heat flux at the elevated temperature of cell operation, the estimation of the maximum work obtainable must consider also a Carnot heat engine receiving the heat flux and operating between the temperature levels of the SOFC and $T_0 = 298.15$ K [25]. This consideration allows the estimation of the ideal first law efficiency of high temperature fuel cells taking into account the magnitude of heat release to environment according to the relation

$$\eta_{\mathrm{I,ideal}} = \frac{-6\mathrm{AHU}(\Delta G)_{\mathrm{T}} + (1 - T_0/T)\dot{Q}_{\mathrm{rejected}}}{-\Delta H_{\mathrm{fuel}}}. \qquad (16)$$

However, when the SOFC is designed to operate autonomously without heat exploitation from a bottoming cycle, the adiabatic SOFC regime is desired.

By considering a desired temperature for the products of the SOFC unit and standard AHU provided by a selected RF and zero-loss burner balance, minimization of heat waste, $\dot{Q}_{\mathrm{rejected}}$, from the SOFC to environment (adiabatic SOFC operation) may be established only if the heat released from hydrogen oxidation is exactly equal to the heat absorbed by the gaseous stream flowing inside the SOFC. In light of this and in absence of cooling media as it is the case of the plant of Fig. 1, the average temperature of the SOFC inlet must be at an appropriately lower value than the prescribed temperature of the products. In this respect, an iterative calculation may be employed as follows

$$Q = \left(T_{\mathrm{sofc,out}} - \frac{T_{\mathrm{sofc,out}} - \Delta T_{\mathrm{sofc}}}{2}\right)\sum_i x_i^s (C_p^s)_i \qquad (17)$$

where Q is given by Eq. (13), $T_{\mathrm{sofc,out}}$ is the desired temperature of the SOFC effluents and ΔT_{sofc} is the unknown optimal temperature difference between the mixture outgoing and incoming the SOFC unit. As follows by Eq. (16), SOFC operation and thus hydrogen oxidation is considered for simplicity to take place in the average temperature between the mixtures downstream and upstream the SOFC.

Following the iterative scheme of Eq. (17), direct minimization of exergy losses due to heat waste from SOFC to environment may be achieved by specifying the optimal temperature difference ΔT_{sofc}, as shown in Fig. 3. Under the assumption of the operation of the ethanol fed plant with RF = 3, $T_{\mathrm{sofc,out}} = 1200$ K and zero-loss burner operation, it is shown that exergy losses due to heat waste decrease with the increment of ΔT_{sofc} and an optimal temperature difference is specified at 332 K. At this optimal case, the heat released by hydrogen oxidation is equal to the heat absorbed by the gaseous mixture in the SOFC and, therefore, thermal impact to environment is eliminated. For a given reforming factor and zero-loss burner balance, this method of ‘‘direct

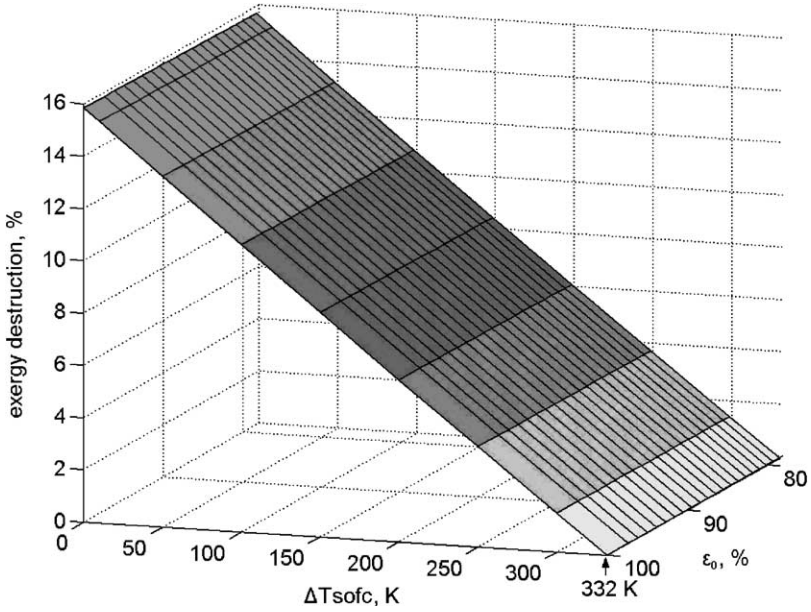

Fig. 3. Direct minimization of thermal exergy losses due to waste heat from the SOFC to environment at zero-loss burner conditions (RF = 3, $T_{sofc,out}$ = 1200 K).

minimization of exergy losses'' from the SOFC, provides the higher possible exergetic efficiency of the plant, as shown in Fig. 4. As observed, by attaining the optimal temperature difference of ΔT_{sofc} = 332 K, exergetic efficiency tends to maximize at 66.5% due to reduction of the average temperature of hydrogen oxidation in the SOFC stack.

3.3. Allocation of irreversibilities

In the two previous sections, a strategy of decision making for the optimization of the overall exergetic efficiency of the plant of Fig. 1 has been provided according to considerations of the first law of thermodynamics. Here, the crucial role of ''exergy analysis'' will be discussed, by contemplating all possible optimally efficient regimes and specifying the best one according to objective criteria such as cost-effectiveness and thermodynamic feasibility.

On the assumption of ideal thermal exchange between the air and reformate streams incoming the SOFC unit, there are infinite temperature combinations of these streams given by the equation

$$T_{ref} = T_{sofc,in} + \frac{\dot{m}_{air}\sum_i x_i^e (C_p^e)_i}{\dot{m}_{ref}\sum_i x_i^r (C_p^r)_i}(T_{air} - T_{sofc,in}) \quad (18)$$

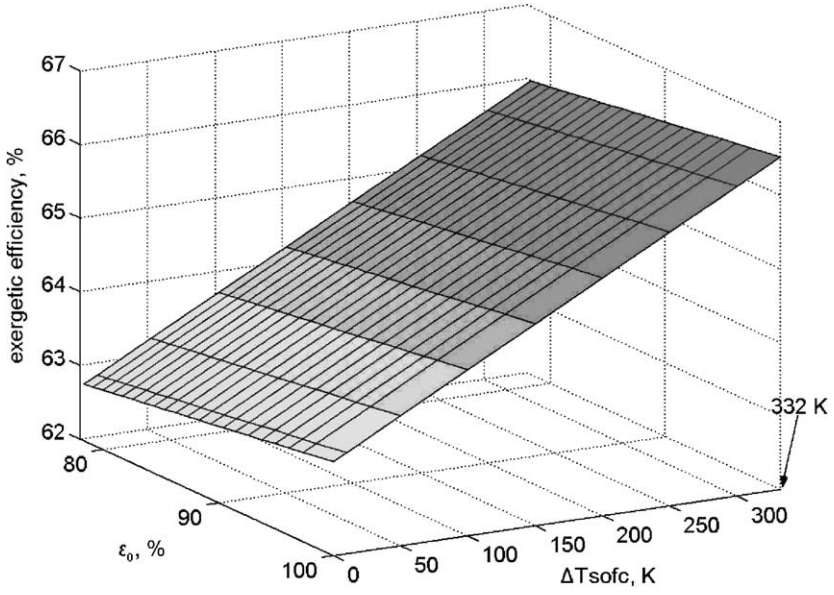

Fig. 4. Effect of thermal losses from the SOFC on the overall exergetic efficiency (RF = 3, $T_{sofc,out}$ = 1200 K).

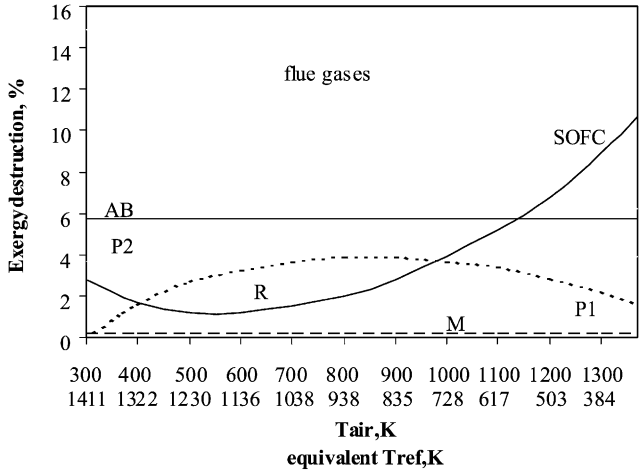

Fig. 5. Allocation of irreversibilities in the units of the optimally designed SOFC plant (RF = 3, $T_{sofc,out}$ = 1200 K, $\Delta T_{sofc} = T_{sofc,in} - T_{sofc,out}$ = 332 K, ε_0 = 100%, U_0 = 78.95%, η_{II} = 66.52%, M: mixer, P1: preheater 1, P2: preheater 2, AB: after burner, R: reformer) at all equivalent schemes for temperatures of preheated air and reformate.

that are providing the same work output (efficiency). Accordingly, the first law analysis is unable to specify an optimal operative scheme regarding the temperatures of the reforming reaction and air preheating. For the example under consideration, this can be done by application of the "exergy analysis" as shown in Fig. 5. In this case, the design parameters of the temperatures of the reformate, T_{ref}, and air preheating, T_{air}, may be specified according to the necessity for cost-effective plant operation, allocating the exergy costs (irreversibilities) of the individual units of the plant. Although the overall exergy destruction rate is constant, different equivalent scenarios of Fig. 5 result in different allocations of exergy costs in the devices of the plant.

Independently on the type of the specific devices that comprise a plant, it has been proved [14] that avoidable exergy destruction in a device of a plant that is close to the final product (i.e. electrical power) has greater impact on the system efficiency and cost of electricity than avoidable exergy destruction of the same magnitude in a device close to the inputs (i.e. fuel, air, steam). Since the major devices that contribute on electricity generation are the reformer and the SOFC, a scenario of low exergy costs in these units is preferable than a scenario involving low exergy costs in devices close to the plant inputs. In this respect, the region of minimal exergy destruction in the SOFC unit may be considered as optimal in terms of cost effectiveness, implying moderate air preheating at 500–650 K and reformate production at 1100–1230 K. Although ethanol reforming has been found feasible at significantly lower temperatures (about 600 K) [20–26], it is here proved that the plant design should aim at the desired value of extent of reforming ε_0 at this specified temperature interval.

To better justify the decision of this optimal region of operation conditions, another reason may also be stated. Fig. 5 implies that minimization of exergy destruction in the SOFC is mainly compensated by an increment of the exergy loss accompanying the stream of flue gases. Although exergy destruction due to dissipative phenomena (friction, chemical reactions, heat transfer, Ohmic losses, etc.) is irreversibly lost, exergy losses may be considered exploitable by an appropriate engine (gas turbines, heat engines, etc.) or useful for practical purposes (heating rooms, water, etc.). As a result, the conditions of minimum exergy destruction in the SOFC are justified again as optimal for engineering rationalism.

Fig. 6 provides an optimal configuration of the ethanol fueled plant (RF = 3, $T_{sofc,out}$ = 1200 K) as result of the above analysis with T_{air} = 625 K and T_{ref} = 1112 K. As it is

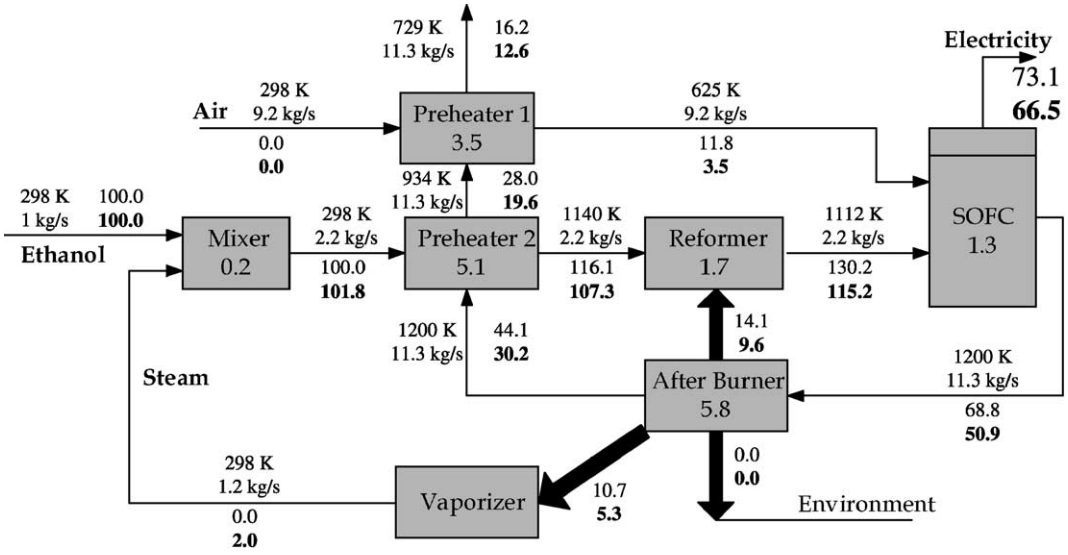

Fig. 6. Optimal configuration of the SOFC plant. RF = 3, 100% theoretical air, ε_0 = 100%, U_0 = 79.85% (plain text stands for energy values while bold stands for exergy ones).

observed, the stream of the exhaust gases with temperature 729 K contains 12.6% of the standard chemical exergy of ethanol and obviously may be useful for practical purposes as mentioned previously. Further, the major exergy sink of the plant is found to be the afterburner with exergy destruction rate equal to 5.8% due to highly irreversible mechanisms that are accompanying all spontaneous combustion processes. However, it is reminded that this rate of exergy destruction in the burner is the minimum possible for the example under consideration, since AHU maximization according to Section 3.1 is practically equivalent to minimization of the participation of combustion in the plant. Finally, the demand for high temperatures of steam reforming reflects into an appreciably high rate of exergy destruction (5.1%) in preheater 1 which is attributed to increased stream-to-stream heat transfer over a finite temperature difference.

3.4. Effect of RF, ΔH_{loss} and $T_{sofc,out}$

When designing the operational parameters of a fuel cell system, one of the most important considerations deals with the possibility of preventing the equipment from destructive effects such as fouling of channels and poisoning or breakdown of catalysts. In the case of the SOFC, carbon deposition is the primary danger to be avoided by an appropriate adjustment of the steam/fuel molar ratio, RF, in the reformer feedstream. According to previous theoretical studies [26,27], the reforming factor (RF) of the ethanol reforming reaction must always be higher than 2.68 when it is accomplished in the temperature range of 800–1200 K. In fact, this value represents the minimum reforming factor above which carbon deposition is thermodynamically impossible at 800 K. At higher temperatures, lower reforming factors can be used but in the present study this value was considered as the minimum possible overestimating the possibility of carbon formation.

The dependence of the attainable energetic and exergetic efficiencies of the ethanol fueled plant mentioned above on the burner balance and the reforming factor may be clarified by the nomograph of Fig. 7. An increment of the heat losses from the afterburner reduces the upper limit of the AHU value and concomitantly has the same effect on both the efficiencies. Similarly, an increase of the reforming factor is also unfavorable in terms of efficiency. Thus, the lower possible limit imposed either by the stoichiometry of the reforming reaction or the carbonization boundary for ethanol is recommended. Results of Fig. 7 have been derived according to the optimization strategy mentioned above for $\varepsilon = 100\%$ when RF > 3. For RF < 3 there exists a maximum $\varepsilon = \varepsilon_{max}$ due to the stoichiometry of the reforming reaction (i.e. for RF $= 2.68$ it is $\varepsilon_{max} = 89.33\%$).

For the cases presented in Fig. 7, specification of optimal ΔT_{sofc} provides the diagram of Fig. 8. Optimal temperature difference decreases as both reforming factor and burner losses tend to increase. An increment of the reforming factor, obviously increases the thermal capacity of the stream of matter flowing inside the device and thus lowers ΔT_{sofc}. Instead, losses from burner balance decrease the AHU values as showed in Fig. 7 and concomitantly the absolute heat amount produced by hydrogen reaction. Therefore, while a non-linear dependence of ΔT_{sofc} on RF is presented, the dependence on burner losses follows a normal linear behavior.

By reminding the allocation of exergy costs according to Fig. 5, it would be useful to recognize the effect of the

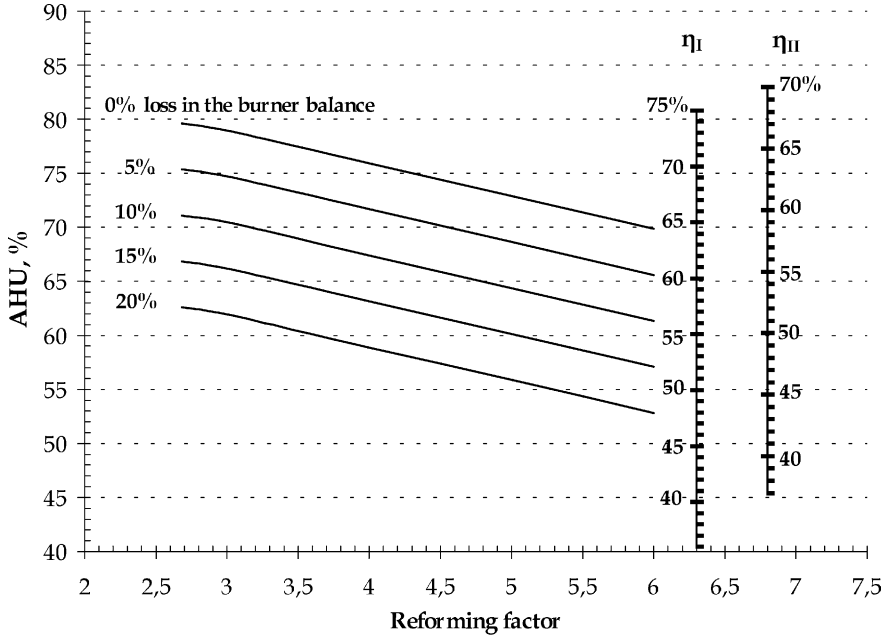

Fig. 7. Nomograph of the first and second law efficiencies for various reforming factors and burner balances ($\varepsilon = \varepsilon_{max}$, optimum ΔT_{sofc}, $T_{sofc,out} = 1200$ K).

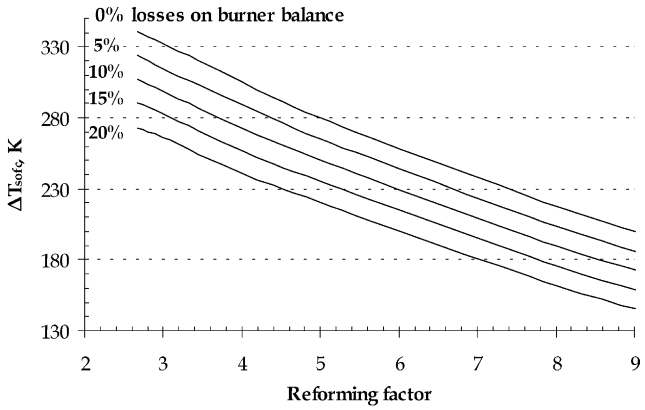

Fig. 8. Effect of RF and burner balance on the optimal temperature difference ΔT_{sofc} required for adiabatic SOFC operation ($T_{sofc,out} = 1200$ K).

reforming factor on the equivalent temperatures of the reformate and air as shown in Fig. 9. Since an increment of the reforming factor induces higher energy requirements from the vaporizer, the zero-loss burner balance (Eq. (12)) provides lower possible AHU values and concomitantly lower plant efficiency. However, the important information from Fig. 9 is that an increment of the reforming factor reduces the slope of Eq. (18) and therefore it also reduces the range of operation conditions that are thermodynamically feasible. For example, when RF = 10, it is shown that air must be preheated up to about 1700 K in order the reforming reaction to take place at about 650–750 K. For such a high temperature of air preheating it is most probable that the exergy analysis will result in one or more devices of the plant with negative exergy destruction rates, expressing a violation of the second law. Especially for the cases of compounds exhibiting high reactivity for reforming at low temperatures (such as ethanol), it is here proved that an increment of the reforming factor is unfavorable, not only due to its effect on efficiency, but also due to suppressing of the range of feasible temperatures for reforming.

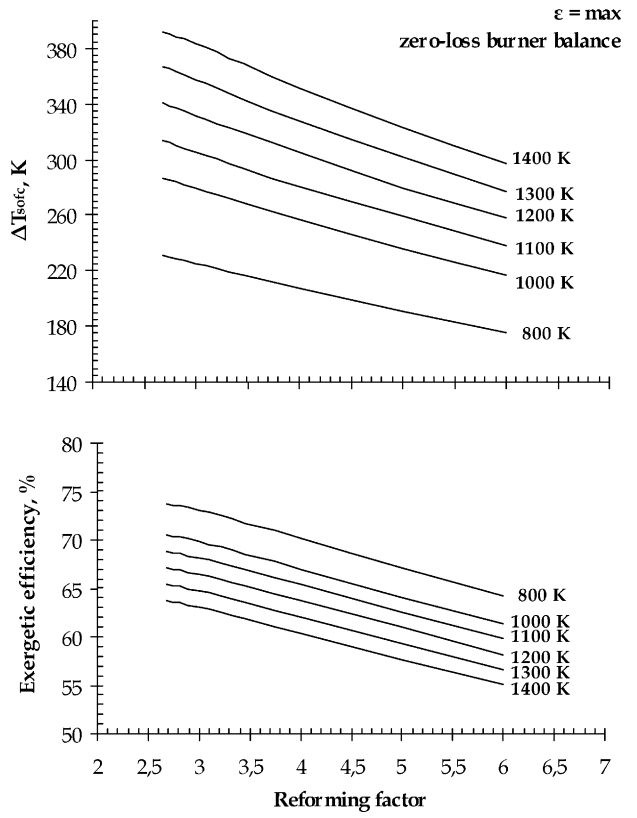

Fig. 10. Effect of the temperature of the SOFC effluents on the optimum ΔT_{sofc} (a) and on the optimum exergetic efficiency (b) of the plant for various reforming factors.

Finally, the methodology mentioned above assumed that the initial design parameter is the temperature of the SOFC effluents, $T_{sofc,out}$. Fig. 10 illustrates the effect of this initial parameter on both the optimal temperature difference of the gaseous mixtures at the outlet and inlet of the SOFC unit and the overall exergetic efficiency of the plant. As one can distinguish, low temperature operating SOFCs require lower temperature differences for direct minimization of exergy

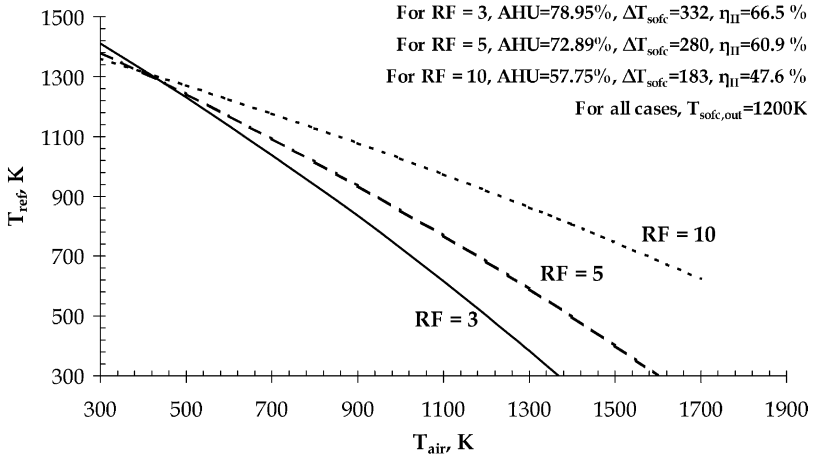

Fig. 9. Equivalent scenarios of temperatures of air preheating and reformate production at various reforming factors.

loss due to waste heat. Further, the theoretical conclusion of Section 3.1 about the incentives for low temperature SOFC operation is confirmed.

4. Conclusions

Energy conversion efficiency of ethanol into electricity was maximized considering a SOFC power plant with external steam reforming, an afterburner, a vaporizer and two heat exchangers. Based on a mathematical model, useful information was deduced about the individual parameters and the independent variables that may lead to optimality according to the first and second law of thermodynamics. It was found that energy conversion optimization is subjected to decisions for the optimization of the burner balance in order to specify the best combination of the extend of the reforming reaction and the hydrogen utilization in the SOFC unit (minimization of combustion participation). Furthermore, an appropriate control of the energy losses from the SOFC was found to be necessary to complete first law optimization. As a consequence, the exergy analysis was applied to provide design criteria in terms of the temperatures of the reforming and air preheating. Allocation of exergy destruction rates was applied to determine optimally controlled unit operations. On the whole, an optimization strategy has been constructed and a thorough examination of the plant operation has been achieved.

References

[1] E. Sciubba, Exergy Int. J. 1 (2001) 68–84.
[2] M.A. Rosen, I. Dincer, Exergy Int. J. 1 (2001) 3–13.
[3] W.R. Dunbar, N. Lior, R.A. Gaggioli, Energy 16 (1991) 1259–1274.
[4] W.R. Dunbar, N. Lior, Combust. Sci. Technol. 103 (1994) 41–61.
[5] J.A. Caton, Energy 25 (2000) 1097–1117.
[6] R. Petela, Fuel Proc. Technol. 67 (2000) 131–145.
[7] J.H. Hirschenhofer, D.B. Stauffer, R.R. Engleman, M.G. Klett, Fuel Cell Handbook, 4th ed., Business/Technology Books, Orinda, USA, 1997.
[8] T.G. Benjamin, E.H. Camara, L.G. Marianowski, Handbook of Fuel Cell Performance, Institute of Gas Technology, Chicago, 1980.
[9] N.Q. Minh, T. Takahashi, Science and Technology of Ceramic Fuel Cells, Elsevier, Amsterdam, 1995.
[10] K.W. Bedringas, The exergy concept in simulation of power systems, Ph.D. thesis, Department of Thermodynamics, University of Trondheim, Trondheim, 1993.
[11] K.W. Bedringas, I.S. Erstevag, S. Byggstoyl, B.F. Magnussen, Energy 22 (1997) 403–412.
[12] S.L. Douvartzides, Ethanol utilization for generation of electricity in solid oxide fuel cells, Ph.D. thesis, University of Thessalia, DMIE, Volos, Greece, 2002 (in English).
[13] T.J. Kotas, The Exergy Method of Thermal Plant Analysis, Butterworths, London, 1985.
[14] A. Bejan, G. Tsatsaronis, M. Moran, Thermal Design and Optimization, Wiley, New York, 1996.
[15] J. Szargut, D.R. Morris, F.R. Steward, Hemisphere, New York, 1988, pp. 297–309.
[16] D.E. Ridler, M.V. Twigg, in: M.V. Twigg (Ed.) Catalyst Handbook, Manson Publishing Ltd., London, 1996 (Chapter 5).
[17] F.J. Marino, E.G. Cerella, S. Duhalde, M. Jobbagy, M.A. Laborde, Int. J. Hydrogen Energy 23 (1998) 1095.
[18] V.V. Galvita, G.L. Semin, V.D. Belyaev, V.A. Semikolenov, P. Tsiakaras, V.A. Sobyanin, Appl. Catal. A: Gen. 220 (2001) 123–127.
[19] S. Cavallaro, S. Freni, Int. J. Hydrogen Energy 21 (1996) 465–469.
[20] A.N. Fatsikostas, D.I. Kontarides, X.E. Verykios, Chem. Commun. (2001) 851–852.
[21] S. Freni, S. Cavallaro, N. Mondello, L. Spadaro, F. Frusteri, J. Power Sources 4704 (2002) 1–5.
[22] S. Freni, N. Mondello, S. Cavallaro, G. Cacciola, V.N. Parmon, V.A. Sobyanin, React. Kinet. Catal. Lett. 71 (1) (2000) 143–152.
[23] S. Freni, J. Power Sources 94 (2001) 14–19.
[24] J.M. Smith, H.C. Van Ness, M.M. Abbott, Introduction to Chemical Engineering Thermodynamics, McGraw-Hill, New York, 1996.
[25] C. Haynes, J. Power Sources 92 (2001) 199–203.
[26] P. Tsiakaras, A. Demin, S. Douvartzides, N. Georgakakis, Ionics 5 (1999) 206–212.
[27] P. Tsiakaras, A. Demin, J. Power Sources 102 (2001) 210–217.